멤브레인(Membrane Journal)
Vol.13, No.3 March, 2003, 143-153

양이온교환막 표면의 전기투석 물분해에서 다가의 큰 이온성분자에 의해 형성된 고정층 바이폴라 계면의 영향

강 문 성 · 최 용 진 · 문 승 현†

광주과학기술원, 환경공학과
(2003년 6월 18일 접수, 2003년 7월 14일 채택)

Effects of Immobilized Bipolar Interface Formed by Multivalent and Large Molecular Ions on Electrodialytic Water Splitting at Cation-Exchange Membrane Surface

Moon-Sung Kang, Yong-Jin Choi, and Seung-Hyeon Moon†

Department of Environmental Science and Engineering, Kwangju Institute of Science & Technology (K-JIST), Gwangju, 500-712, South Korea
(Received June 18, 2003, Accepted July 14, 2003)

요 약: 본 연구에서는 양이온교환막 표면에 형성된 바이폴라 계면이 물분해 현상에 미치는 영향을 조사하였다. 실험결과, 전기투석 중 막표면에 형성된 고정화된 바이폴라 계면이 심각한 물분해를 유발함을 알 수 있었다. 특히, 고정화된 바이폴라 계면은 다가 양이온이 전해질로 이용되는 전기투석 시스템에서 양이온교환막 표면에 쉽게 형성됨을 알 수 있었다. 낮은 용해도적 상수를 갖는 다가 양이온들은 급격한 물분해를 유발하였는데 이는 이들이 막표면에서 쉽게 수산화물의 형태로 침적되며 따라서 수소-친화 그룹과 수산화-친화 그룹으로 구성된 바이폴라 계면이 막-용액 계면에 형성됨을 알 수 있었다. 따라서 물분해는 막 표면의 금속수산화물 층과 막의 고정전하 그룹간에 발생되는 강한 전기장에 의해 크게 활성화됨을 알 수 있다. 또한 이와 유사하게 분자량이 큰 유기 상대이온들이 막표면에 누적되는 경우에도 고정화된 바이폴라 계면이 형성되어 한계전류밀도 이상에서 심각한 물분해를 유발하였다. 따라서 전기투석의 고전류 운전시 효율 향상을 위해서는 막표면에 유발되는 고정화된 바이폴라 계면의 형성을 억제하는 것이 매우 중요함을 알 수 있다.

Abstract: The effects of bipolar interface formed on the surface of cation-exchange membrane on water splitting phenomena were investigated. Results showed that the formation of immobilized bipolar interface resulted in significant water splitting during electrodialysis. In particular, the immobilized bipolar interface was easily created on the cation-exchange membrane surface in the electrodialytic systems where multivalent cations served as an electrolyte. Multivalent cations with low solubility product resulted in violent water splitting because they were easily precipitated on the membrane surface in hydroxide form. Therefore, the bipolar interface consisting of H- and OH-affinity groups were formed on the membrane-solution interface. Apparently, water splitting was largely activated with the help of strong electric fields generated between the metal hydroxide layer and fixed charge groups on the membrane surface. Likewise, the accumulation of large molecular counter ions on the membrane surface led to the formation of a fixed bipolar structure that could cause significant water splitting in the over-limiting current region. Therefore, the prevention of the immobilization of bipolar interface on the membrane surface is very essential in improving the process efficiency in a high-current operation.

Keywords: *Bipolar interface, ion-exchange membrane, water splitting phenomena, multivalent cations, large molecular counter ions*

†주저자(e-mail : shmoon@kjist.ac.kr)

1. 서 론

For many years, electrodialysis (ED) using ion-exchange membranes (IEMs) has been utilized in various applications. Recently, the development of high-performance membranes enabled the use of ED in several industrial applications such as demineralization of whey [1], recovery of metals from metal plating rinse waters [2], recovery of inorganic and organic acids [35], and separation of amino acids from a fermentation broth [6]. To expand the applicable fields of the ED, economic efficiency should clearly be improved. Since the ED processing cost is dominantly dependent on the effective membrane area, operating at the highest practicable current density is essential in getting the maximum ion flux per unit membrane area [7]. However, operating current levels are restricted by the concentration polarization (CP) in such electrical-driven membrane processes.

The limiting current density (LCD) is the maximum current allowed to operate an ED process [8]. If the current exceeds the limiting one, the process efficiency decreases due to the increase in electrical resistance and occurrence of water splitting (WS). In practice, however, loss in the current efficiency and increase in the power consumption due to the WS and CP that occurred on the membrane surface are not significant during the over-limiting current operation [7]. This means that the over-LCD operation may improve the economic effectiveness in electro-membrane processes. Unfortunately, WS and CP behaviors depend predominantly upon the characteristics of the electrolytes used. Earlier studies reported that the water splitting rate drastically increased in electro-membrane systems where Ca^{2+}, Mg^{2+}, and other multivalent cations served as an electrolyte. Water splitting possibly caused the deposition of insoluble metallic residues (*i.e.*, metal hydroxide) on the membrane surface. Therefore, multivalent cations caused significant loss in the current efficiency and increase in power consumption by fouling on the membrane surface [9].

A previous study by the researchers reported that an electrostatic interaction occurred between the fixed charge groups and their hydrated counter ions in the repulsion zone. Therefore, water molecules were possibly polarized and dissociated at the bipolar interface [10]. However, the bipolar interface was unstable due to the electromigration of counter ions through the membrane. Therefore, water splitting in the non-fouled membrane was definitely weaker than that in the membrane with fixed bipolar interface (*e.g.*, membranes fouled with metal hydroxides). Based on these observations, the formation of immobilized bipolar interface is expected to result in significant water splitting. As mentioned earlier, the immobilized bipolar interface is easily created on the cation-exchange membrane surface in the electro-membrane systems where multivalent cations serve as an electrolyte. In addition, large molecular organic ions possibly form the immobilized bipolar interface since they easily accumulate on the membrane surface due to their large molecular size.

In this study, the effects of the immobilized bipolar interface formed on the surface of ion-exchange membrane on WS and CP behaviors were investigated to provide useful information for the efficient over-LCD operation in ED. The effects of ionic valency and molecular size on over-limiting current behaviors in the cation-exchange membrane were systematically studied using various electrochemical characterizations.

2. Experiment

2.1. Materials

For this study, various multivalent cations (*i.e.*, $MaCl_2$, $CaCl_2$, and $FeCl_3$ purchased from Aldrich) and homologous ammonium chlorides ($R\text{-}NH_3Cl$, where $R=CH_3$, $(CH_2)_3CH_3$, $(CH_2)_4CH_3$, and $(CH_2)_5CH_3$, purchased from Acros Organics) in reagents grade were used as electrolytes. Neosepta CMX (cation-exchange membrane, purchased from Tokuyama Corp., Japan) and a highly water-swollen type of poly(vinyl alcohol)/poly(styrene sulfonic acid) (PVA/PSSA) cation-exchange membranes were also used. The detailed preparation procedure for the PVA/PSSA membrane was described

in the previous paper [11].

2.2. Membrane Characterization

The chronopotentiometric and current-voltage (I-V) curves were measured in two-compartment cell experiments [11,12]. Water-splitting capabilities were determined through six-compartment cell experiments [11]. The transport number of the water ions (H^+ and OH^-) generated from the membrane surface was estimated from the change in pH according to:

$$t_{H+} = \frac{FV(\triangle C_{H+}/\triangle t)}{IA} = t_{OH-} = \frac{FV(\triangle C_{OH-}/\triangle t)}{IA} \quad (1)$$

where V is the volume of the solution, F the Faraday constant, $C_{H+/OH-}$ the concentration of proton/hyroxyl ion, t the time, I the current density, and A the membrane area. The detailed experimental procedures were described in the previous papers [11,12].

2.3. Sulfonated Poly(ether sulfone) Cation-Exchange Membrane

Sulfonated poly(arylene ether sulfone) (S-PSU) was prepared using the traditional post-sulfonation route for impedance study. Poly(arylene ether sulfone) (base polymer, PSU, Udel® P-1700, Amoco), chlorosulfonic acid (sulfonating agent, CSA, Aldrich), and 1,1,2,2-tetrachloroethane (solvent, TCE, Aldrich) were utilized without further purifications. PSU was dried in a vacuum oven at 130°C for 8 hr prior to use. The dried PSU (26.6 g, 0.056 mole) was dissolved in 190 g TCE in a 500-mL 4-neck flask fitted with mechanical stirrer, condenser, and nitrogen sparge tube. The solution was purged with nitrogen for an hour, with CSA (8.39 g, 0.072 mole) subsequently added dropwise for 20 min. The reaction was continued for 2.0 hr at room temperature. The reaction solution was then added dropwise over an hour to 1,000 mL of vigorously stirred methanol. The precipitated polymer was washed with cold water and methanol. It was then dried overnight in a vacuum oven at 100°C. Finally, the dried S-PSU was dissolved in *N*-methyl-2-pyrrolidone (NMP) as 25 wt.%.

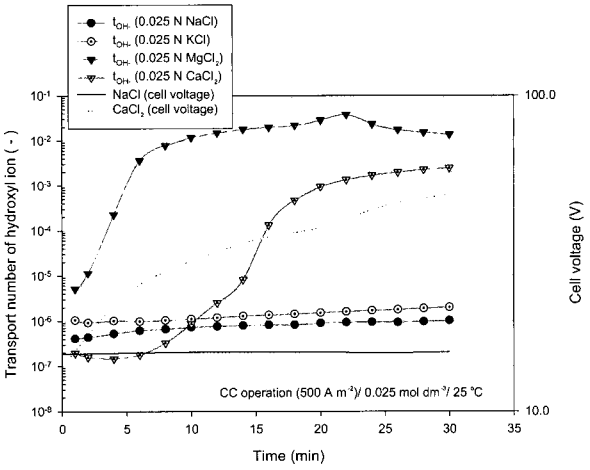

Fig. 1. Variations in transport number of hydroxyl ions and cell voltage of the CMX membrane contacting with various electrolyte solutions.

2.4. Impedance Analysis

Impedance measurements were made with a computer-controlled potentiostat/galvanostat (PGSTAT30, AutoLab, Eco Chemie BV, Netherlands) equipped with a rotating disk electrode system (RDE 628, Metrohm Ltd., Switzerland). The working electrode was a 3-mm diameter platinum electrode (Metrohm Ltd., Switzerland). An Ag/AgCl electrode (Metrohm Ltd., Switzerland) was used as the reference electrode, while a glassy carbon rod electrode (Metrohm Ltd., Switzerland) was utilized as the counter electrode. The platinum disk electrode was coated with a thin S-PSU layer using a spin coater (KW-4A, Chemat Tech., INC., USA). Sodium chloride (0.010 mol dm^{-3}) was used as an electrolyte. Impedance measurements were carried out in 10^{-3}-10^6 Hz frequency range with an electrode rotating rate of 2,000 rpm and 0.1 mV amplitude. All experiments were carried out at room temperature under a nitrogen atmosphere.

3. Results and Discussion

3.1. Effects of Multivalent Cations

Fig. 1 shows the variations in the transport number

of hydroxyl ions and cell voltage for the CMX membrane in contact with various electrolyte solutions. The water-splitting experiments were carried out at a constant current (500 A m^{-2}) for 30 min. In the monovalent ion (*i.e.* Na^+ and K^+) solutions, little difference in the transport numbers was observed. The cell voltages also did not change during the tests. For the divalent ions (Mg^{2+} and Ca^{2+}), however, significant increases in the pH and cell voltage were evident. Note that the divalent cations easily precipitate as hydroxide form [13].

$$Mg(OH)_{2(s)} \Leftrightarrow Mg^{2+} + 2OH^-; \quad \log K_{so} = -10.74 \quad (2)$$

$$Ca(OH)_{2(s)} \Leftrightarrow Ca^{2+} + 2OH^-; \quad \log K_{so} = -5.3 \quad (3)$$

The solubility product K_{so} of Mg^{2+} ($K_{so,Mg} = 1.82 \times 10^{-11}$) was smaller than that of Ca^{2+} ($K_{so,Ca} = 5.01 \times 10^{-6}$). Therefore, the precipitation of $Mg(OH)_2$ on the membrane surface takes place more easily. Jialin *et al.* classified the metal hydroxides as OH-affinity groups and the sulfonic acid groups (SO_3^-) as H-affinity groups [14]. They presumed that the bipolar interface consisting of H- and OH-affinity groups enhances the prepolarization of water molecules before they dissociate under the influence of strong electric fields. Based on the results of this study, however, the bipolar structure consisting of the hydroxide residues (OH-affinity group) and the fixed charge groups (H-affinity group) increased the water splitting and the membrane resistance drastically.

Major factors contributing to the enhancement in water splitting by metal hydroxides may be: (i) increase in the electric fields generated between the metal hydroxides and membrane surface; (ii) catalytic water splitting reactions between metal hydroxides (or metal ions) and water molecules [9,15]; (iii) retardation of the transport of counter ions through the membrane; (iv) increase in water activity (*i.e.*, enhancement of interface hydrophilicity) [16], and; (v) increase in the looseness of water bonds [14,17]. These factors seemed to contribute complexly to the water-splitting mechanism. In light of the chemical reaction model, the possible catalytic reactions (for iron(III) hydroxide) at the membrane-metal hydroxide interface are as follows [18]:

(In basic condition)

$$M(H_2O)_3(OH)_{3(s)} + H_2O \Leftrightarrow M(H_2O)_2(OH)_4^- + H_3O^+ \quad (4)$$

$$M(H_2O)_2(OH)_4^- + H_2O \Leftrightarrow M(H_2O)_3(OH)_{3(s)} + OH^-. \quad (5)$$

In the reaction equations, M is a multivalent ion, e.g., Fe^{3+} or Cr^{3+}. From the pC-pH relations for hydroxo iron(III) complexes [13], these reactions possibly occur in basic conditions near the boundary region of the immobilized metal hydroxide layer. Since water splitting occurs at the interface between the metal hydroxides and fixed charge groups (*i.e.*, sulfonic acid groups), the side near the metal hydroxide layer may be in basic condition due to the transport of hydroxyl ions generated. Therefore, the reactions under basic conditions are seemingly dominant in this case. Moreover, the water splitting reactions reversibly proceed according to Eqs. (4) and (5) due to the electromigration of the dissociated ions (H^+ and OH^-) out of the reaction layer under the reverse bias condition.

After the desalting experiments, changes in electrochemical properties of the membranes were evaluated through the I-V and chronopotentiometric curves (**Fig. 2**). **Tables 1** and **2** list the characteristic values of the I-V and chronopotentiometric curves (measured in 0.025 mol dm^{-3} NaCl), respectively. The fraction of the conducting region for each ion-exchange membrane was determined using the modified Sand equation proposed by Choi *et al.* [12] with the following formula:

$$\varepsilon = \frac{2i\tau^{1/2}(\overline{t_k} - t_k)}{C_0 z_k F(\pi D)^{1/2}} \quad (6)$$

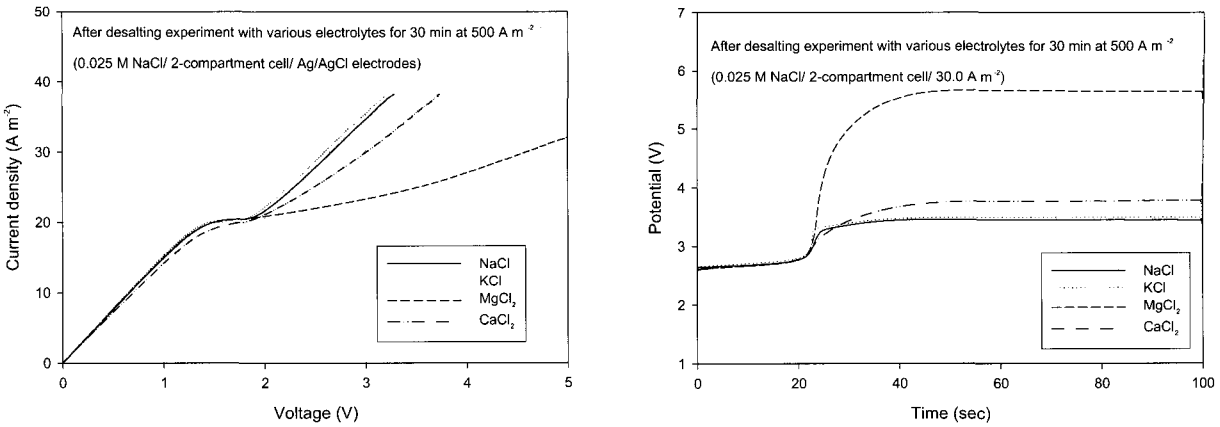

(a) (b)

Fig. 2. I-V and chronopotentiometric curves of the CMX membrane. (a) I-V curves; (b) Chronopotentiometric curves

Table 1. Characteristic Values of I-V Curves (CMX Membrane)

Electrolyte	NaCl	KCl	$MgCl_2$	$CaCl_2$
R_{1st} (Ωcm^2)	695.2	682.3	707.5	715.0
R_{3rd} (Ωcm^2)	771.0	757.3	3767.2	1066.0
R_{3rd}/R_{1st} (-)	1.11	1.11	5.32	1.49
Rinc. (%)	10.9	11.0	432.5	49.1
V (V)	0.52	0.52	0.66	0.73
LCD (A m^{-2})	19.98	19.89	20.08	18.43

Table 2. Characteristic Values of Chronopotentiometric Curves (CMX Membrane)

Electrolyte	NaCl	KCl	$MgCl_2$	$CaCl_2$
Transition time, τ (sec)	21.75	22.12	22.38	20.32
I τ 1/2	13.66	14.11	14.19	13.52
Transport No. (-)*	1.009	1.004	1.000	1.030
Transport No. (-)**	0.992	0.992	0.923	0.963
Fraction of conducting region, ε (-)	0.972	0.981	0.872	0.894

where is the fraction of conducting region, i the current density, τ the transition time, C_o the concentration of electrolyte, z_k the valence of k ion, F the Faraday constant, and D the diffusion coefficient of electrolyte (NaCl). $\overline{t_k}$, t_k are the transport numbers of k ion in the membrane and solution phase, respectively. The transition time (τ) was determined using the intersection of the tangents with the first and second stages of the curve (**Fig. 2** (b)). For the calculation of the values, the diffusion coefficient (1.61×10^{-5} cm^2 sec^{-1}) of NaCl and the transport number (0.396) of Na^+ ion in the solution phase were obtained from literature [19].

By incorporating the apparent transport numbers for each membrane into Eq. (6), the values were calculated. The electrical properties of the CMX membrane significantly changed due to the deposition of the hydroxide residues after the desalting experiments. The bipolar structure formed on the membrane surface diminished the fixed charge densities. As a result, the electroconvective effects decreased (*i.e.* increases in ΔV and R_{3rd}/R_{1st} values). The decrease in the values according to the precipitation of metal hydroxides was also an indication of reduction in the net surface charge densities on the membrane surface. Although the surface charge density decreased, the fixed bipolar structure formed on the membrane surface drastically increased the water-splitting capabilities of the membrane. Water splitting was seemingly activated mainly with the help of strong electric fields generated between the metal hydroxide layer and fixed charge groups on the membrane surface.

3.2. Impedance Analyses

The rotating disk electrode (RDE) is an effective tool for the study of electrochemical systems because the fluid flow is well defined. Likewise, the uniform axial velocity yields a uniform mass-transfer-limited current density [20,21]. Liquid flows are generated in the solution when the electrode rotates around its vertical axis. The liquid flow impinges on the electrode

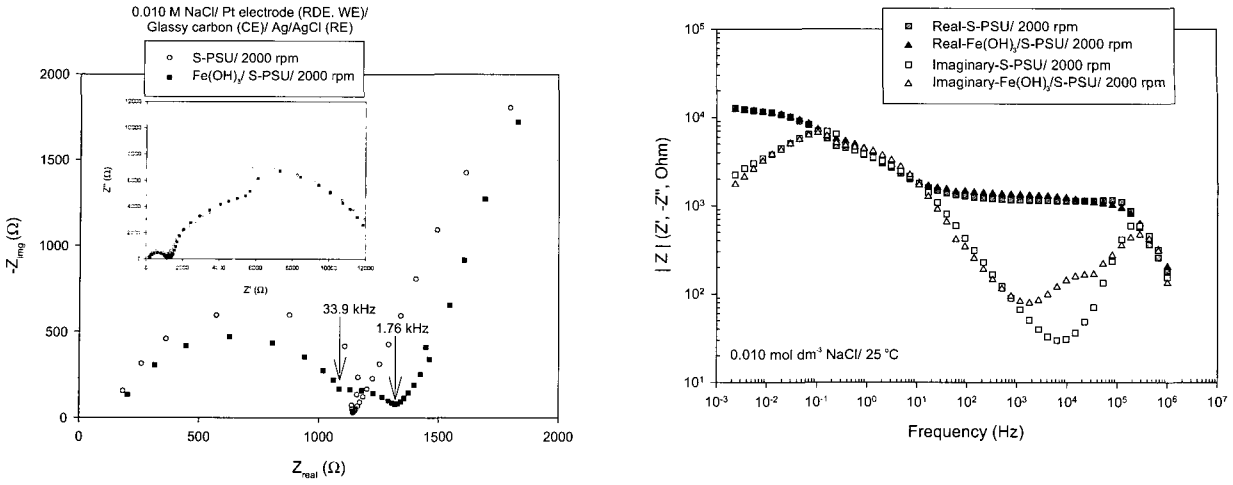

(a) (b)

Fig. 3. Impedance plots for the S-PSU membranes. (a) Nyquist plots; (b) Impedances according to the frequency

in the center of the rotating disk. It is subsequently diverted by centrifugal forces to the periphery [22]. Turbulent liquid flows developing at such electrodes give rise to thinner diffusion layers. In practice, the RDE system has been used for the impedance analysis [23,24]. In particular, Park *et al.*, reported the impedance characteristics of a rotating disc electrode coated with a sulfonated polysulfone cation-exchange membrane [23]. They showed that the impedance response was mostly dependent upon the content of sulfonic acid groups ($-SO_3^-H^+$) in the membrane.

In this study, impedance measurements were conducted to investigate the changes in the membrane surface properties through the deposition of metal hydroxides (*i.e.*, $Fe(OH)_3$). For the deposition of $Fe(OH)_3$, the S-PSU membrane (thickness = 1-3 μm, ion-exchange capacity = 1.10 meq./ g) coated on the platinum disk electrode was immersed in a 0.25 mol dm^{-3} $FeCl_3$ aqueous solution for one day. It was then allowed to come into contact with a 0.1 mol dm^{-3} NaOH solution for an hour. After washing in distilled water, the metal hydroxide deposited S-PSU/Pt electrode was stored in a 0.5 mol dm^{-3} NaCl solution for more than a day.

Fig. 3 shows the impedance plots measured in a 0.010 mol dm^{-3} NaCl with the rotating speed of 2,000 rpm. The differences in the impedance responses were observed in the 33.9 - 1.76 kHz frequency range. For

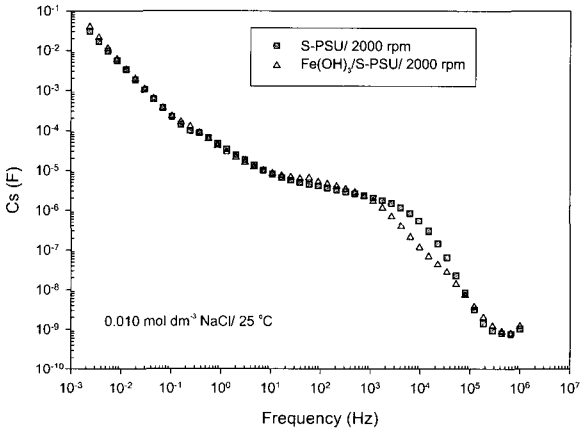

Fig. 4. Serial capacitances according to the frequency.

the metal hydroxide deposited S-PSU, **Fig. 3** (a) shows an impedance plot with two partially overlapping "sunken semicircles" that can be observed for the two-layer composite membrane [25]. This observation confirms that the metal hydroxide layer was formed on the membrane surface, resulting in a distinguishable bilayer structure.

As shown in **Fig. 3** (b), the imaginary part (Z") of the impedances was affected by the deposition of metal hydroxides ($Fe(OH)_3$) in the 33.91.76 kHz frequency range, while the real part was not. Note that the imaginary part of the impedances was assigned to the capacitance in the membrane [26]. Moreover, the serial capacitances C_s (shown in **Fig. 4**) calculated from the

Table 3. Characteristics of Cations Having Various Molecular weights

Electrolyte	Mw of cation (g mol^{-1})	Ionic diffusivity (cm^2 sec^{-1})	Transport number in water (-)
Sodium chloride (NaCl)	23.0	1.33 E-5	0.397
Methylamine hydrochloride (CH_3NH_2-HCl)	32.1	1.43 E-5	0.414
Propylamine hydrochloride($CH_3(CH_2)_2NH$-HCl)	60.1	1.33 E-5	0.328
Butylamine hydrochloride(($C_2H_5)_2NH$-HCl)	74.1	8.93 E-6	0.305
Hexylamine hydrochloride($CH_3(CH_2)_5NH_2$-HCl)	102.2	7.73 E-6	0.276

Table 4. Transport Numbers in Membrane Contacting with Electrolytes Having Various Molecular Weights (Measured by emf method (0.001 / 0.005 mol dm^{-3} NaCl))

Membrane	CMX (WSR=27%)	PSSA (WSR=60%)	PSSA (WSR=165%)
Sodium chloride (NaCl)	0.99	0.97	0.82
Methylamine hydrochloride (CH_3NH_2-HCl)	0.99	0.97	0.85
Propylamine hydrochloride ($CH_3(CH_2)_2NH$-HCl)	0.99	0.98	0.87
Butylamine hydrochloride (($C_2H_5)_2NH$-HCl)	0.99	0.98	0.92
Hexylamine hydrochloride ($CH_3(CH_2)_5NH_2$-HCl)	0.95	0.98	0.93

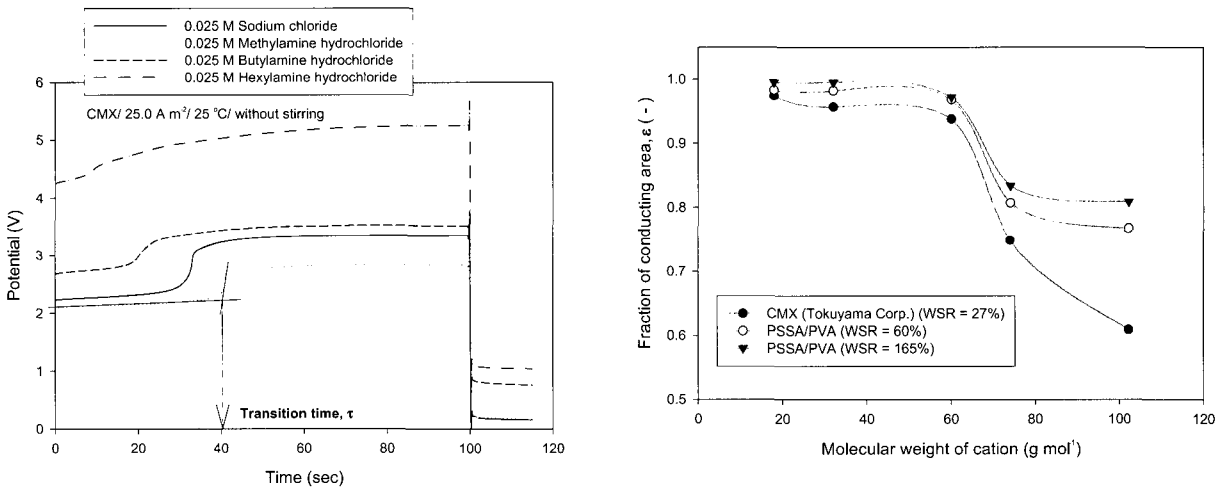

(a) (b)

Fig. 5. Chronopotentiometric curves measured in amine-hydrochloride solutions having different molecular weights and fractions of conducting region according to molecular weight of cation. (a) Chronopotentiometric curves in various amine-hydrochloride solutions; (b) Fractions of conducting region according to ionic molecular weights

admittance data also decreased due to the deposition of $Fe(OH)_3$ in the same frequency range. C_s was believed to decrease due to the reduction in the membrane net surface charge density by the deposited-metal hydroxides with positive charge property.

3.3. Molecular Sieving Effects

To investigate the influences of the degree of cross-linking on water splitting, cation-exchange membranes with varying water swelling ratios were tested with different amine hydrochloric acids (**Table 3**). The highly water-swollen cation-exchange membranes were prepared using water-soluble poly(vinyl alcohol) (PVA) and poly (styrene sulfonic acid) (PSSA) as the base materials [11]. The degree of cross-linking was controlled through chemical cross-linking with a glutaraldehyde solution.

Table 4 shows the transport numbers of counter ions in various ammonium chlorides. **Fig. 5** (a) shows the chronopotentiometric curves of the CMX membrane measured with various amine hydrochlorides. The

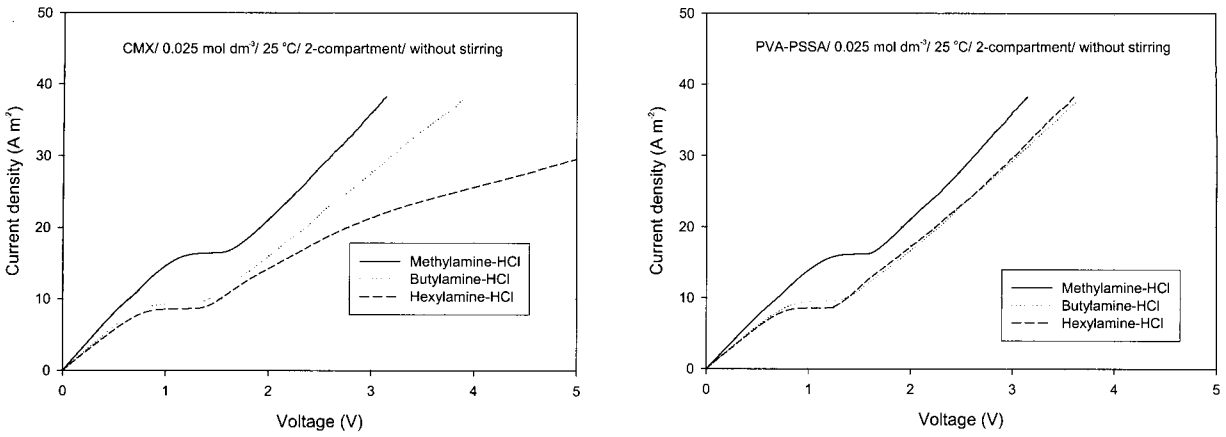

(a) (b)

Fig. 6. I-V curves of the CMX and PSSA membranes measured in amine-hydrochloride solutions having different molecular weights. (a) CMX membrane; (b) PSSA membrane

potential levels and transition times varied according to the diffusivity and transport numbers in the bulk solution and the membrane. The fractions of the conducting region (ε) were determined with the transition time (τ) in the chronopotentiometric curve and presented in **Fig. 5** (b). The values decreased given the increase in the molecular size of counter ions (especially when over 60 g mol^{-1}); thus indicating that the large molecular ions accumulated on the membrane surface since the free volume of the membrane was smaller than the size of the ions [27]. The values for the fractions of conducting regions increased in the following order: CMX (WSR=27%) PSSA (WSR=60%) PSSA (WSR= 165%). These differences were even greater when larger ions were tested.

The I-V curves for the CMX and PSSA membranes are shown in **Fig. 6**. For the CMX membrane, the I-V response measured in a 0.025 mol dm^{-3} hexylamine-HCl solution had abnormally high voltage increase in the over-LCD region. This indicates that the hexylamine-H^+ ions (Mw=102.2 g mol^{-1}) that accumulated on the membrane surface retarded ion transport and increased membrane resistance. On the other hand, the I-V curve for the PSSA membrane showed a typical response, even for the hexylamine hydrochloride solution.

Fig. 7 shows the transport numbers for the hydroxyl ion measured in amine-hydrochloride solutions with

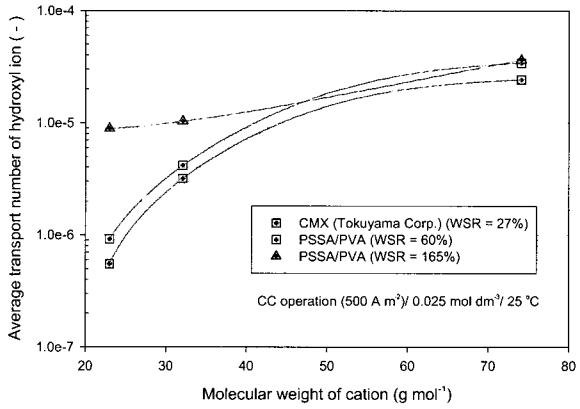

Fig. 7. Transport numbers of hydroxyl ion measured in amine-hydrochloride solutions having different molecular weights.

different molecular weight ions. As shown in this figure, the transport numbers for the hydroxyl ion (Eq. (1)) increased given an increase in the molecular weight of the cations for all membranes tested. The water splitting capabilities had the following trend in a NaCl solution: CMX (WSR=27%) PSSA (WSR=60%) PSSA (WSR=165%). Note that the water swelling property (or WSR) is dominantly dependent on the content of the fixed charge groups and the influence of the fixed charge density on water splitting. The relative increment of water splitting was evaluated by:

$$R_{B/A} = \left(\frac{J_B - J_A}{J_A} \right) \times 100(\%) \quad (7)$$

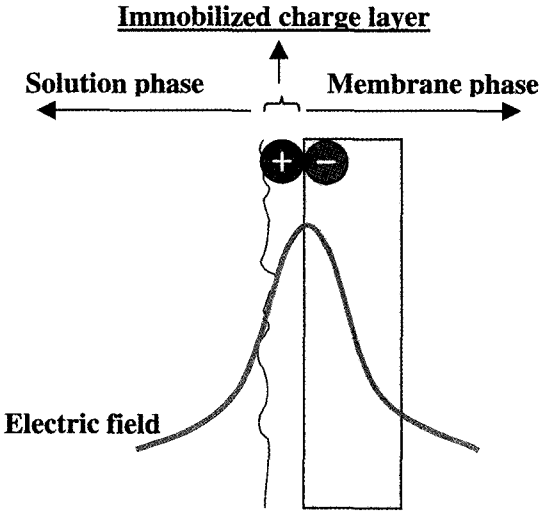

Fig. 8. Electric fields generated on the interface between immobilized charge layer and membrane.

Table 5. Increase Rates of Water Splitting Fluxes in Membranes Contacting with Electrolytes Having Various Molecular Weights (Na= sodium; MA=methyl ammonium; BA=butyl ammonium ions)

Membrane	CMX (WSR=27%)	PSSA (WSR=60%)	PSSA (WSR=165%)
$R_{MA/Na}$ (%)	475.1	351.6	16.3
$R_{BA/Na}$ (%)	4294.2	3621.4	310.9

where $R_{B/A}$ is the increase rate of water splitting, J_A the water splitting flux in electrolyte A, and J_B the water splitting flux in electrolyte B. According to the H^+ and OH^- fluxes seen in NaCl solution, the increment of water splitting was calculated and the results shown in **Table 5**. Water splitting significantly increased given an increase in the molecular weight of the ions, and the order was PSSA (WSR=165%) PSSA (WSR=60%) CMX (WSR=27%). This order indicates that the accumulation of the counter ion with larger molecular size than the free volume size of the membrane took place on the membrane surface. Therefore, a fixed bipolar structure was instantly created on the solution-membrane interface. Consequently, the fixed bipolar structure formed on the membrane surface drastically increased the water-splitting effect with the help of the strong electric fields. The electric fields generated on the interface between the immobilized charge layer (formed by multivalent and large molecular cations) and membrane surface are schematically drawn in **Fig. 8.** The strong electric fields generated at the immobilized bipolar interface are seemingly the most important factor dominating water splitting and electroconvective behaviors.

4. Conclusions

The effects of the immobilized bipolar interface formed on the surface of ion-exchange membrane on water splitting phenomena were investigated. Water splitting drastically increased when multivalent cations were used as an electrolyte, indicating that the formation of an immobilized bipolar structure in the membrane-solution interface significantly accelerated water splitting. Apparently, water splitting was largely activated with the help of strong electric fields generated between the metal hydroxide layer and fixed charge groups on the membrane surface. The molecular sieving on the membrane surface was also confirmed as the most important parameter dominating the water-splitting behavior when large molecular ions were used as an electrolyte. The accumulation of counter ions with large molecular size on the membrane surface induced the formation of a fixed bipolar structure, which could cause significant water splitting when over the LCD. As a result, the inhibition of immobilized bipolar interface was very important in enhancing current efficiency and reducing energy consumption for the over-LCD operations in electrodialysis. This may be achieved by removing multivalent cations prior to the operation and utilizing the membranes with high free volume for the separation of large molecular organic ions.

Acknowledgments

This work was supported by the National Research Laboratory (NRL) Program of Korea Institute of Science and Technology Evaluation and Planning (Project No. 2000-N-NL-01-C-185).

References

1. Batchelder, B. T., Electrodialysis applications in whey processing, *FIL-IDF Bulletin,* **212** (1987) 84.
2. Itoi, S., I. Nakamura, and T. Kawahara, Electrodialytic recovery process of metal-finishing wastewater, *Desalination,* **32** (1980) 383.
3. Boniardi, N., R. Rota, G. Nano, and B. Mazza, Lactic acid production by electrodialysis Part 1: Experimental tests, *J. Appl. Electrochem.*, **27** (1997) 125.
4. Novalic, S., F. Jagschits, J. Okwor, and K. D. Kulbe, Behavior of citric acid during electrodialysis, *J. Membr. Sci.,* **108** (1995) 201.
5. Lee, E.-G., Moon, S.-H., Chang, Y.-K., Yoo, I.-K., and Chang, H.-N., Lactic acid recovery using two-stage electrodialysis and its modeling, *J. Membr. Sci.*, **145** (1998) 53.
6. Kim, Y.-H. and Moon, S.-H., Lactic Acid Recovery from Fermentation Broth Using One-stage Electrodialysis, *J. Chem. Technol.and Biotechnol.*, **176** (2001) 1.
7. Choi, J.-H., Transport phenomena in ion-exchange membranes at under- and over-limiting current regions, Ph.D thesis, K-JIST (Korea), 2002.
8. Makai A.J. and J.C.R. Turner, Electrodialysis at high current density using a laboratory stack, *Trans IChemE*, **60** (1982) 88.
9. Shel'deshov, N.V., Zabolotskii, V.I., and Ganych, V.V., Water dissociation rate at cation-exchange membrane: Influence of insoluble metal hydroxides, *Russian J. Electrochem.* **30**(12) (1994) 1458.
10. Kang, M.-S., Water-Splitting Phenomena and Applications in Ion-Exchange Membranes, Ph.D thesis, K-JIST (Korea), 2003.
11. Kang, M.-S., Choi, Y.-J., and Moon, S.-H., Water swollen cation-exchange membranes prepared using PVA(polyvinyl alcohol)/PSSA-MA(polystyrene sulfonic acid-co-maleic acid), *J. Membr. Sci.*, **207**(2) (2002) 157.
12. Choi, J.-H., Kim, S.-H., and Moon, S.-H., Heterogeneity of ion-exchange membranes: The effects of membrane heterogeneity on transport properties, *J. Colloid & Interf. Sci.*, **241** (2001) 120.
13. Snoeyink, V.L. and Jenkins, D., *Water chemistry*, John Wiley & Sons, Inc., New York, 1980.
14. Jialin, L., Yazhen, W., Changying, Y., Guangdou, L., and Hong, S., Membrane catalytic deprotonation effects, *J. Membr. Sci.*, **147** (1998) 247.
15. Simons, R., Water splitting in ion exchange membranes, *Electrochim. Acta*, **30**(3) (1985) 275.
16. Simons, R., Preparation of a high performance bipolar membrane, *J. Membr. Sci.*, **78** (1993) 13.
17. Hanada, F., Hirayama, K., Ohmura, N., and Tanaka, S., Bipolar membrane and method for its production, US Patent 5,221,455, 1993.
18. Kang, M.-S., Tanioka, A., and Moon, S.-H., Effects of Interface Hydrophilicity and Metallic Compounds on Water-Splitting Efficiency in Bipolar Membranes, *Korean J. Chem. Eng.*, **19**(1) (2002) 99.
19. Crow, D. R., *Principles and Applications of Electrochemistry*, 4th Ed., Blackie Academic & Professional, London, 1994.
20. Durbha, M. and Orazem, M.E., Current distribution on a rotating disk electrode below the mass-transfer-limited current, *J. Electrochem. Soc.*, **145**(6) (1998) 1940.
21. Fedkiw, P. S., Song, S., Sharma, S., and Ye, J.-H., Coulometry of a mass-transfer limited reaction with a membrane-covered rotating disk electrode, *J. Electrochem. Soc.*, **142**(6) (1995) 1909.
22. Bagotzky, V. S., *Fundamentals of Electrochemistry*, Plenum Press, New York, 1993.
23. Park, S.-Y., Lee, J.-W., Jang, S.-H., Kim, L.-H., Choi, D.-K., and Joe, Y.-I., Impedance characteristics of a rotating disc electrode coated with a sulfonated polysulfone cation-exchange membrane, *J. Power Sources*, **83** (1999) 217.
24. Orazem, M. E., Durbha, M., Deslouis, C., Takenouti, H., and Tribollet, B., Influence of surface phenomena on the impedance response of

a rotating disk electrode, *Electrochim. Acta*, **44** (1999) 4403.

25. Srensen, T. S. (Ed.), *Surface Chemistry and Electrochemistry of Membranes*, Marcel Dekker, Inc., New York, 1999.
26. Starzak, M. E., *The Physical Chemistry of Membranes*, Academic Press, San Diego, 1984.
27. Choi, J.-H. and Moon, S.-H., Pore size characterization of cation-exchange membranes by chronopotentiometry using homologous amine ions, *J. Membr. Sci.*, **191** (2001) 225.